

# Nonlinear Enhancement of Chiroptical Response through Subcomponent Substitution in $M_4L_6$ Cages\*\*

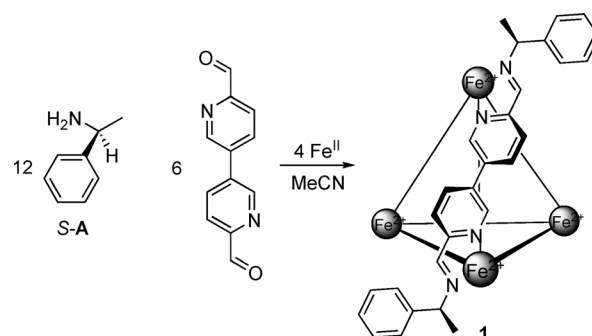
Naoki Ousaka, Jack K. Clegg, and Jonathan R. Nitschke\*

Metal–organic cages<sup>[1]</sup> can provide chiral inner phases<sup>[2,3]</sup> for enantioselective guest recognition and sensing<sup>[2]</sup> as well as stereoselective transformations.<sup>[3]</sup> Further development in this area requires new chiral capsules, both to provide well-defined chiral void spaces for new stereoselective transformations, and as testbeds for fundamental studies of chirotopic spaces.<sup>[4]</sup> Recently, we have reported the preparation of tetrahedral  $M_4L_6$  cages<sup>[5]</sup> utilizing subcomponent assembly.<sup>[6]</sup> These cages, assembled from octahedral metal ions and  $C_2$ -symmetric bis(bidentate) ligands, have been observed to form racemic mixtures of homochiral structures, in which each of the four metal centers has the same stereogenic configuration. This observation implies strong cooperative stereochemical coupling between metal centers,<sup>[1c,3a,5e,7]</sup> i.e., a situation in which it is energetically favorable for metal centers of one configuration ( $\Delta$  or  $\Lambda$ ) to have neighbors of the same configuration. This phenomenon has its conceptual roots with Pfeiffer,<sup>[8]</sup> who was first to demonstrate that metal-centered chiroptical properties can be influenced by stereocenters elsewhere within a system. Recent work has elucidated different factors that can modulate the strength of this coupling, allowing cages with mixed metal configurations to be prepared.<sup>[5e,9]</sup>

Cooperative interactions between stereogenic centers lead to nonlinear enhancements in chiroptical properties, which have been widely studied in helical polymers<sup>[10]</sup> and other (macro-) supramolecular systems.<sup>[11]</sup> In these cases, the helical bias is amplified either in the presence of small amounts of segments of defined stereochemistry (sergeants-and-soldiers effect),<sup>[10–12]</sup> or where one enantiomeric conformation predominates to only a small degree (majority rules).<sup>[10,11,13]</sup> Here we demonstrate how subcomponent self-assembly can allow metal–organic capsules to be prepared in enantiopure form through the incorporation of chiral amine building blocks,<sup>[14]</sup> providing a platform for the exploration of the degree to which stereochemical information can be transmitted from one part of a complex structure to another.

The cage framework for this study was constructed from twelve primary amines (which were incorporated as imines), six equivalents of 6,6'-diformyl-3,3'-bipyridine, and four  $Fe^{II}$  ions. As previously reported,<sup>[5c]</sup> the amine subcomponents of the cage are arrayed on its periphery and can be substituted by more electron-rich amines. Thus, a cage-to-cage conversion should take place through substitution of aromatic amines by aliphatic amines.<sup>[15]</sup> (*S*)-1-phenylethylamine (*S*-A) has been observed to engender both diastereoselectivity (metal configuration) and regioselectivity (*facial* coordination) in mononuclear  $Fe^{II}$  tris(pyridylimine) complexes through steric and  $\pi$ -stacking effects.<sup>[14]</sup>

$Fe_4L_6$  cage **1** was prepared from *S*-A, 6,6'-diformyl-3,3'-bipyridine and iron(II) triflate [ $Fe(OTf)_2$ ] in  $CH_3CN$  (Scheme 1).



**Scheme 1.** Diastereoselective formation of tetrahedral  $Fe_4L_6$  cage **1**. Only one ligand is drawn for clarity.

ESI-MS and NMR measurements are consistent with **1** adopting a solution structure analogous to its structure in the solid state, as revealed by single-crystal X-ray analysis (Figure 1). In the crystal, **1**, which crystallizes in the chiral space group  $P4_122$ , is shown to possess the expected tetrahedral geometry with  $\Delta$  configurations at all metal centers. The absolute configuration and enantiopurity of the sample was confirmed by anomalous dispersion effects. Each pyridine ring is observed to  $\pi$ -stack with a phenyl ring on a neighboring ligand, as indicated by centroid–centroid distances of 3.5–3.8 Å. Similar  $\pi$ -stacking was observed in a related mononuclear complex.<sup>[14]</sup> A disordered partial-occupancy triflate counteranion is observed within the central cavity of **1** in the crystal.

The high-symmetry structure of **1** is reflected in its simple  $^1H$  NMR spectrum (Figure 2). The NOESY spectrum of **1** revealed long-range NOEs between protons on the pyridine and benzene rings (Supporting Information, Figure S1),

[\*] Dr. N. Ousaka, Dr. J. K. Clegg, Dr. J. R. Nitschke  
University of Cambridge, Department of Chemistry  
Lensfield Road, Cambridge, CB2 1EW (UK)  
E-mail: jrn34@cam.ac.uk  
Homepage: <http://www-jrn.ch.cam.ac.uk>

[\*\*] This work was supported by a JSPS postdoctoral fellowship for young scientists (no. 2692), the European Research Council, and the Marie Curie IIF Scheme of the 7th EU Framework Program. We thank Dr. M. M. J. Smulders for his comments on the manuscript and the EPSRC Mass Spectrometry Service at Swansea for conducting FT-ICR MS experiments.

Supporting information for this article is available on the WWW under <http://dx.doi.org/10.1002/anie.201107532>.

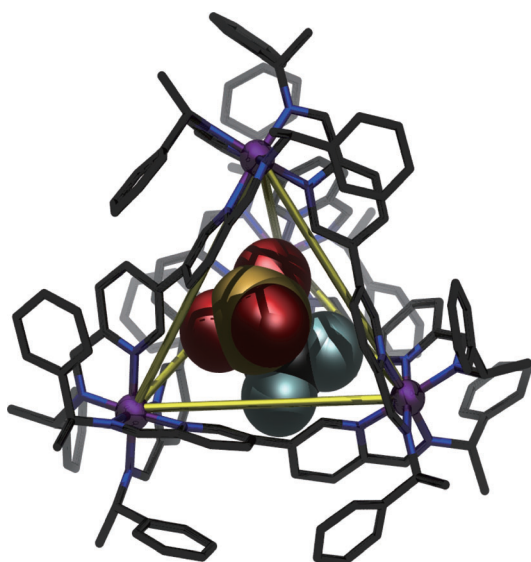


**Figure 1.** The crystal structure of cage  $\Delta\Delta\Delta\Delta$ -1. Only one of two orientations of the disordered  $\text{OTf}^-$  anion inside **1** is shown.

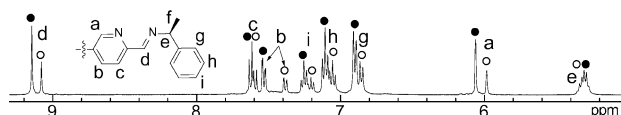
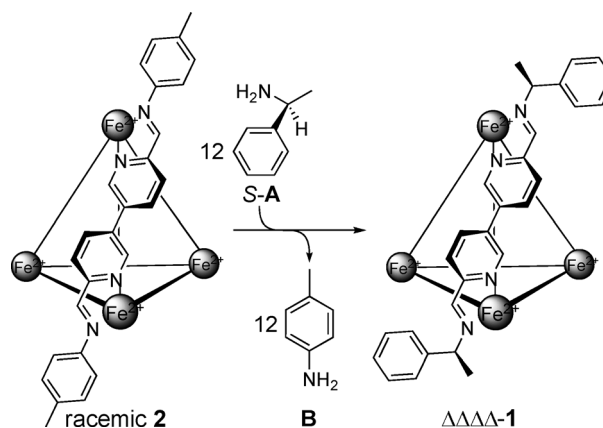


**Figure 2.**  $^1\text{H}$  NMR spectrum (400 MHz) of **1** in  $\text{CD}_3\text{CN}$  at  $27^\circ\text{C}$ :  $[\text{1}] = 2.0 \times 10^{-3} \text{ M}$ . The filled and empty circles denote  $\text{OTf}^- \subset \text{1}$  and empty cage **1**, respectively.

consistent with  $\pi$ -stacking in solution analogous to what was observed in the solid state (Figure 1). Two distinct sets of  $^1\text{H}$  NMR signals were observed, however, indicating the presence of two species in solution. The ratio between these two species was sensitive to changes in temperature, with one of the two sets of signals decreasing with increasing temperature and disappearing above  $70^\circ\text{C}$  (Figure S2), returning to its prior intensity as the temperature was lowered again. The intensity of this set of signals increased following addition of excess (127 equiv) tetrabutylammonium triflate (Figure S3). Based upon these results, the two sets of signals could be assigned to **1** encapsulating one  $\text{OTf}^-$  ion inside its cavity ( $\text{OTf}^- \subset \text{1}$ ), and empty **1**.<sup>[16]</sup> The  $^{19}\text{F}$  NMR spectrum of **1** also showed two signals at  $-76.9$  and  $-78.4$  ppm corresponding to encapsulated and free  $\text{OTf}^-$ , respectively (Figure S4).

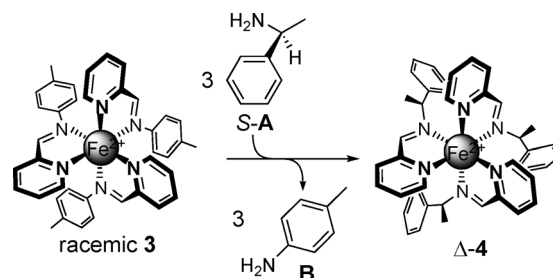
The CD spectrum of **1** showed intense split-type Cotton effects centered at 570 and 295 nm, indicating the diastereoselective formation of the same  $\Delta\Delta\Delta\Delta$ -isomer (**S-1**) (Figure S5) in solution that was observed in the solid state (Figure 1).<sup>[14,17]</sup> The enantiomer of **1**, prepared from *R*-**A** (*R*-**1**), showed the expected mirror-image CD spectrum. The optical activity of **1** did not change even after heating to  $70^\circ\text{C}$  for 2 days.

As shown in Scheme 2, treatment of racemic **2** with *S*-**A** resulted in conversion into optically active **1** through subcomponent substitution. The reaction's progress could be followed by observing the disappearance of *S*-**A** and the



**Scheme 2.** Conversion from the optically inactive **2** to optically active **1** by subcomponent substitution.

appearance of free *p*-toluidine **B** over 40 h at  $70^\circ\text{C}$  by  $^1\text{H}$  NMR spectroscopy (Figure S6). The conversion of model complex **3** to  $\Delta$ -**4**<sup>[14]</sup> also occurred under similar conditions (Scheme 3).



**Scheme 3.** Conversion from the optically inactive mononuclear complex **3** to optically active **4** by subcomponent substitution.

Estimation of the amounts of partially substituted cages and complexes containing different proportions of *S*-**A** and **B** residues during the substitution reactions was not feasible due to the complexity of their NMR spectra. These spectra (Figure S7) were not consistent with the selective desymmetrization<sup>[4]</sup> that would accompany cooperativity in the substitution of the **B** residues of **2**. An example of selective desymmetrization would be the preferential substitution of all three aniline residues at one corner of **2**, leading to the formation of a cage with approximate  $C_3$  point symmetry. Such a cage would have characteristic and interpretable NMR spectra,<sup>[5]</sup> in contrast to the complex spectra observed.

The detection of all 13 possible constitutionally distinct products (containing different numbers of **A** and **B** residues) by ESI-MS following the addition of *S*-**A** (6 equiv) to **2** (Figure S8) also lends support to our inference of non-selective substitution of **B** by **A** within **2**.

Based on the success of these transformations through subcomponent substitution, we carried out sergeants-and-soldiers experiments involving the reactions of **2** and **3** with different quantities of *S*-**A** to obtain partially substituted complexes, where the sergeants and soldiers are *S*-**A** and **B**

residues, respectively (Scheme S1 and S2).<sup>[18]</sup> CD intensities measured at 610 and 321 nm for **2** and at 600 and 290 nm for **3** increased nonlinearly with increasing *S-A* content (Figure 3 and S9a). In addition, the absorbances at 355 nm for **2** and

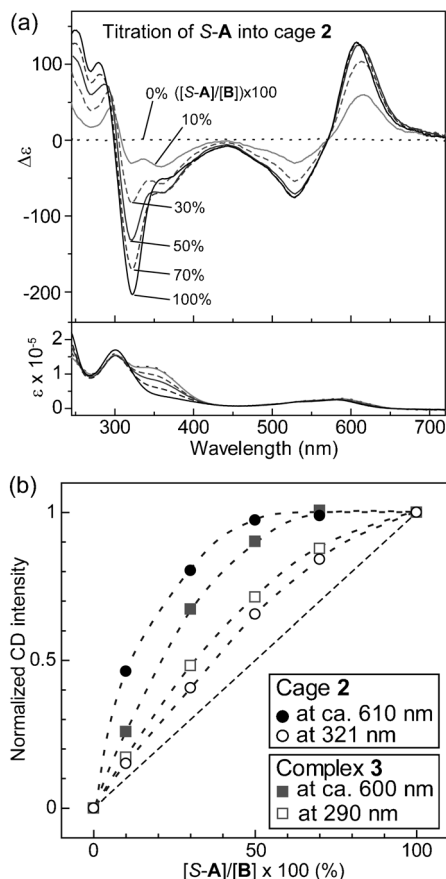


**Figure 3.** a) CD (top) and absorption spectra (bottom) of **2** with different amounts of *S-A* in CD<sub>3</sub>CN/CH<sub>3</sub>CN (1:10, v/v) at 20 °C: [2]<sub>0</sub> = 9.7 × 10<sup>−5</sup> M, data are presented for [B]/[S-A] values ranging from 1:0 to 1:1. b) Plots of normalized CD intensities at 610 (filled circle) and 321 nm (open circle) for **2** with *S-A* as a function of *S-A* content. CD and absorption spectra of **3** with different amounts of *S-A* are shown in Figure S9a.

327 nm for **3** decreased due to the decreased  $\pi$ -conjugation length in the ligands of **1** and **4** as compared to **2** and **3**. The magnitude of nonlinear effects measured at 321 nm is smaller than those at 610 nm because CD intensities around 321 nm are sensitive to inter-ligand exciton coupling, where CD and absorption spectral patterns in this region are different to each another.<sup>[19]</sup> In contrast, the metal-to-ligand charge transfer (MLCT) absorptions of all iron complexes in this study, at 610 nm, are of comparable intensities. Moreover, the CD intensity had already reached its maximum value by the point at which 50% *S-A* had been incorporated, indicating that the CD MLCT intensities of cages having different proportions of *S-A* track the proportion of metal centers in the  $\Delta$  configuration in excess of those having a  $\Delta$  configuration and are not affected by the proportion of *S-A* vs. *B* residues present in the product. We therefore used the

intensity of the CD signal at the MLCT transition to gauge the proportion of excess  $\Delta$ -configuration metal centers present within a given sample of cages.

The observation that the CD intensity was at almost half its maximum value (Figure 4), despite 42% of intact **2** remaining in the <sup>1</sup>H NMR spectrum in the presence of 10%

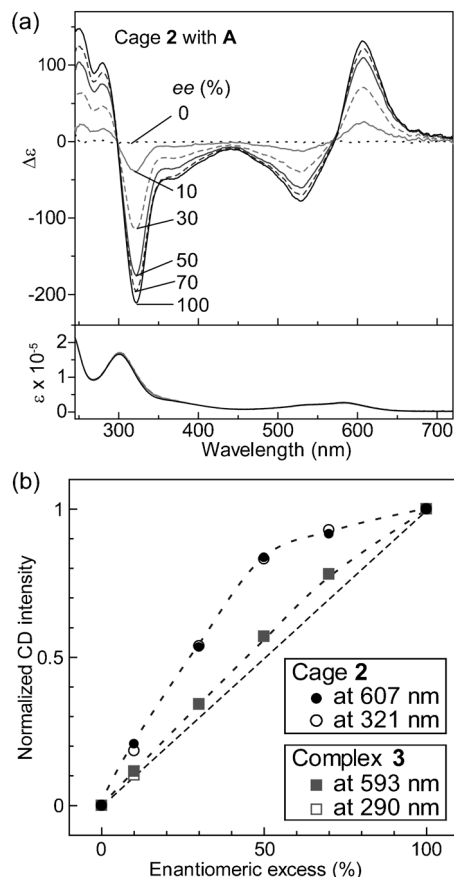


**Figure 4.** a) CD (top) and absorption spectra (bottom) of **2** with *A* (*ee* = 0–100%, *S*-rich) in CD<sub>3</sub>CN/CH<sub>3</sub>CN (1:10, v/v) at 20 °C: [2]<sub>0</sub> = 9.7 × 10<sup>−5</sup> M, [B]/[A] = 1:1. b) Plots of normalized CD intensities at 607 (red circle) and 321 nm (blue circle) for **2** with *A* and at 593 (green square) and 290 nm (orange square) for **3** with *A* as a function of the % *ee* of *A*. CD and absorption spectra of **3** with *A* (*ee* = 0–100%, *S*-rich) are shown in Figure S9b.

*S-A* content (1.2 equiv per **2**) (Figure S7), implies that approximately two *S-A* subcomponents are enough to induce all of a cage's Fe<sup>II</sup> stereocenters to adopt the same configurational twist. Additionally, the CD intensity was observed to have reached its maximum value when the signals of intact **2** were observed to have almost disappeared in the <sup>1</sup>H NMR spectrum (50% *S-A* content) (Figure S7). In the case of mononuclear complex **3**, similar trends were observed, with a smaller nonlinear effect. The difference in sergeants-and-soldiers nonlinearity between **2** and **3** is directly attributable to the degree to which the bipyridine linkers mediate cooperative stereochemical communication between the four metal centers in **2**, an effect which must be absent in mononuclear **3**.

To elucidate the influence of subcomponent configuration on cage formation, *R,S*-**1**, prepared from racemic *R,S*-**A**, was prepared and characterized. Its  $^1\text{H}$  NMR spectrum proved complex, with no peaks observed for homochiral *S*- or *R*-**1** (Figure S10), and did not change after heating at 70°C for 2 days. Although the NMR spectra could not be interpreted readily,  $\text{Fe}_4\text{L}_6$  species were clearly observed by ESI-MS (Figure S11). Thus, complete chiral self-sorting did not occur in this system.<sup>[20]</sup> However, a tendency was observed towards configurational sorting at each metal center. This was supported by the results for the model complex *R,S*-**4**, wherein the major products were homochiral  $\Delta$ - and  $\Lambda$ -**4** (53%) as determined by  $^1\text{H}$  NMR integration (Figure S12). These results are consistent with *S*- and *R*-**A** incorporating into the cages with a small bias for vertices containing three identical subcomponents.

When cage **2** was allowed to react with *R,S*-**A** having different degrees of enantiomeric excess (*ee*), cage **1** was formed in which the *ee* of the amine subcomponent was amplified (majority rules experiments; Scheme S3 and S4) in its influence on metal configurational excess. The CD intensities increased nonlinearly with the increasing % *ee* of **A**, also without change to the UV/Vis absorption intensity (Figure 4). In contrast, mononuclear model complex *R,S*-**4**, prepared by subcomponent substitution from **A** having different degrees of *ee* showed a weaker nonlinear effect due, again, to the lack of ligand-mediated cooperative stereochemical communication (Figure 4b and S9b).<sup>[21]</sup>

In conclusion, we have demonstrated the diastereoselective subcomponent self-assembly of a new  $\text{M}_4\text{L}_6$  cage, and observed amplification in chiroptical response in both the cage and a related mononuclear complex. In addition, we observed a greater amplification in the case of the tetranuclear cage complex than the mononuclear analog, reflecting the presence of cooperative communication between metal centers. These findings may help elucidate the intricate mechanisms by which stereochemical information is transmitted between the subunits of complex supramolecular architectures, and also to provide new methods for the construction of diastereomerically pure cages enveloping large spaces for the chiral separations and transformations of guests.

CCDC 849335 contains the supplementary crystallographic data for this paper. These data can be obtained free of charge from The Cambridge Crystallographic Data Centre via [www.ccdc.cam.ac.uk/data\\_request/cif](http://www.ccdc.cam.ac.uk/data_request/cif).

Received: October 25, 2011

Revised: December 5, 2011

Published online: December 30, 2011

**Keywords:** cage compounds · diastereoselectivity · sergeant-and-soldiers · stereochemical information transfer · supramolecular chemistry

- [1] a) M. D. Ward, *Chem. Commun.* **2009**, 4487–4499; b) P. Jin, S. J. Dalgarno, J. L. Atwood, *Coord. Chem. Rev.* **2010**, 254, 1760–1768; c) R. W. Saalfrank, H. Maid, A. Scheurer, *Angew. Chem.* **2008**, 120, 8924–8956; *Angew. Chem. Int. Ed.* **2008**, 47, 8794–

- 8824; d) W. Meng, B. Breiner, K. Rissanen, J. D. Thoburn, J. K. Clegg, J. R. Nitschke, *Angew. Chem.* **2011**, 123, 3541–3545; *Angew. Chem. Int. Ed.* **2011**, 50, 3479–3483; e) R. Chakrabarty, P. S. Mukherjee, P. J. Stang, *Chem. Rev.* **2011**, 111, 6810–6918; f) C. R. K. Glasson, J. K. Clegg, J. C. McMurtrie, G. V. Meehan, L. F. Lindoy, C. A. Motti, B. Moubaraki, K. S. Murray, J. D. Cashion, *Chem. Sci.* **2011**, 2, 540–543; g) J. K. Clegg, F. Li, K. A. Jolliffe, G. V. Meehan, L. F. Lindoy, *Chem. Commun.* **2011**, 47, 6042–6044.
- [2] a) X. X. Zhang, J. S. Bradshaw, R. M. Izatt, *Chem. Rev.* **1997**, 97, 3313–3362; b) J. M. Rivera, T. Martin, J. Rebek, *Science* **1998**, 279, 1021–1023; c) T. Ishi-i, M. A. Mateos-Timoneda, P. Timmerman, M. Crego-Calama, D. N. Reinhoudt, S. Shinkai, *Angew. Chem.* **2003**, 115, 2402–2407; *Angew. Chem. Int. Ed.* **2003**, 42, 2300–2305; d) D. Fiedler, D. H. Leung, R. G. Bergman, K. N. Raymond, *J. Am. Chem. Soc.* **2004**, 126, 3674–3675; e) T. Liu, Y. Liu, W. Xuan, Y. Cui, *Angew. Chem.* **2010**, 122, 4215–4218; *Angew. Chem. Int. Ed.* **2010**, 49, 4121–4124.
- [3] a) D. Fiedler, D. H. Leung, R. G. Bergman, K. N. Raymond, *Acc. Chem. Res.* **2005**, 38, 349; b) A. Nakamura, Y. Inoue, *J. Am. Chem. Soc.* **2005**, 127, 5338–5339; c) Y. Nishioka, T. Yamaguchi, M. Kawano, M. Fujita, *J. Am. Chem. Soc.* **2008**, 130, 8160; d) M. Yoshizawa, J. K. Klosterman, M. Fujita, *Angew. Chem.* **2009**, 121, 3470–3490; *Angew. Chem. Int. Ed.* **2009**, 48, 3418–3438.
- [4] K. Mislow, J. Siegel, *J. Am. Chem. Soc.* **1984**, 106, 3319–3328.
- [5] a) P. Mal, D. Schultz, K. Beyeh, K. Rissanen, J. R. Nitschke, *Angew. Chem.* **2008**, 120, 8421–8425; *Angew. Chem. Int. Ed.* **2008**, 47, 8297–8301; b) P. Mal, B. Breiner, K. Rissanen, J. R. Nitschke, *Science* **2009**, 324, 1697–1699; c) Y. R. Hristova, M. M. J. Smulders, J. K. Clegg, B. Breiner, J. R. Nitschke, *Chem. Sci.* **2011**, 2, 638–641; d) I. A. Riddell, M. M. J. Smulders, J. K. Clegg, J. R. Nitschke, *Chem. Commun.* **2011**, 47, 457–459; e) W. Meng, J. K. Clegg, J. D. Thoburn, J. R. Nitschke, *J. Am. Chem. Soc.* **2011**, 133, 13652–13660.
- [6] J. R. Nitschke, *Acc. Chem. Res.* **2007**, 40, 103–112.
- [7] a) D. L. Caulder, K. N. Raymond, *Acc. Chem. Res.* **1999**, 32, 975–982; b) C. R. K. Glasson, G. V. Meehan, C. A. Motti, J. K. Clegg, P. Turner, P. Jensen, L. F. Lindoy, *Dalton Trans.* **2011**, 40, 10481–10490; c) D. F. Perkins, L. F. Lindoy, A. McAuley, G. V. Meehan, P. Turner, *Proc. Natl. Acad. Sci. USA* **2006**, 103, 532–537; d) S. P. Argent, T. Riis-Johannessen, J. C. Jeffery, L. P. Harding, M. D. Ward, *Chem. Commun.* **2005**, 4647–4649.
- [8] a) P. Pfeiffer, K. Quehl, *Chem. Ber.* **1932**, 65, 560–565; b) S. Kirschner, N. Ahmad, *J. Am. Chem. Soc.* **1968**, 90, 1910–1911.
- [9] R. W. Saalfrank, H. Maid, A. Scheurer, R. Puchta, W. Bauer, *Eur. J. Inorg. Chem.* **2010**, 2903–2906.
- [10] a) M. M. Green, N. C. Peterson, T. Sato, A. Teramoto, R. Cook, S. Lifson, *Science* **1995**, 268, 1860–1866; b) M. M. Green, J.-W. Park, T. Sato, A. Teramoto, S. Lifson, R. L. B. Selinger, J. V. Selinger, *Angew. Chem.* **1999**, 111, 3328–3345; *Angew. Chem. Int. Ed.* **1999**, 38, 3138–3154; c) J. J. L. M. Cornelissen, A. E. Rowan, R. J. M. Nolte, N. A. J. M. Sommerdijk, *Chem. Rev.* **2001**, 101, 4039–4070; d) M. Fujiki, *Macromol. Rapid Commun.* **2001**, 22, 539–563; e) E. Yashima, K. Maeda, H. Iida, Y. Furusho, K. Nagai, *Chem. Rev.* **2009**, 109, 6102–6211.
- [11] a) M. A. Mateos-Timoneda, M. Crego-Calama, D. N. Reinhoudt, *Supramol. Chem.* **2005**, 17, 67–79; b) A. R. A. Palmans, E. W. Meijer, *Angew. Chem.* **2007**, 119, 9106–9126; *Angew. Chem. Int. Ed.* **2007**, 46, 8948–8968; c) D. Pijper, B. L. Feringa, *Soft Matter* **2008**, 4, 1349–1372; d) T. F. A. De Greef, M. M. J. Smulders, M. Wolffs, A. P. H. J. Schenning, R. P. Sijbesma, E. W. Meijer, *Chem. Rev.* **2009**, 109, 5687–5754.
- [12] M. M. Green, M. P. Reidy, R. J. Johnson, G. Darling, D. J. O'Leary, G. Willson, *J. Am. Chem. Soc.* **1989**, 111, 6452–6454.
- [13] M. M. Green, B. A. Garetz, B. Munoz, H. Chang, S. Hoke, R. G. Cooks, *J. Am. Chem. Soc.* **1995**, 117, 4181–4182.



- [14] a) S. E. Howson, L. E. N. Allan, N. P. Chmel, G. J. Clarkson, R. J. Deeth, A. D. Faulkner, D. H. Simpson, P. Scott, *Dalton Trans.* **2011**, 40, 10416–10433; b) S. E. Howson, L. E. N. Allan, N. P. Chmel, G. J. Clarkson, R. van Gorkum, P. Scott, *Chem. Commun.* **2009**, 1727–1729.
- [15] D. Schultz, J. R. Nitschke, *J. Am. Chem. Soc.* **2006**, 128, 9887–9892.
- [16] A binding constant for the encapsulation of OTf<sup>−</sup> within the cavity of **1** is ca. 140 M<sup>−1</sup>, which is approximately two orders of magnitude smaller than that of **2**.<sup>[Sc]</sup> This is attributed to the presence of more electron density on the cage walls in **1** than that of **2** probably due to a combination of a decreased  $\pi$ -conjugation length in **1** and also the greater nucleophilicity of S-**A** compared to **B**.
- [17] U. Knof, A. Von Zelewsky, *Angew. Chem.* **1999**, 111, 312–333; *Angew. Chem. Int. Ed.* **1999**, 38, 302–322.
- [18] N. Ousaka, Y. Takeyama, H. Iida, E. Yashima, *Nat. Chem.* **2011**, 3, 856–861.
- [19] a) M. Ziegler, A. von Zelewsky, *Coord. Chem. Rev.* **1998**, 177, 257–300; b) S. G. Telfer, N. Tajima, R. Kuroda, *J. Am. Chem. Soc.* **2004**, 126, 1408–1418.
- [20] a) W. Jiang, A. Schäfer, P. C. Mohr, C. A. Schalley, *J. Am. Chem. Soc.* **2010**, 132, 2309–2320; b) K. Osowska, O. S. Miljanić, *J. Am. Chem. Soc.* **2011**, 133, 724–727; c) M. M. Safont-Sempere, P. Osswald, M. Stolte, M. Grüne, M. Renz, M. Kaupp, K. Radacki, H. Braunschweig, F. Würthner, *J. Am. Chem. Soc.* **2011**, 133, 9580–9591; d) K. Osowska, O. S. Miljanić, *Synlett* **2011**, 1643–1648; e) K. Osowska, O. S. Miljanić, *Angew. Chem.* **2011**, 123, 8495–8499; *Angew. Chem. Int. Ed.* **2011**, 50, 8345–8349.
- [21] K. I. Arias, E. Zysman-Colman, J. C. Loren, A. Linden, J. S. Siegel, *Chem. Commun.* **2011**, 47, 9588–9590.